W. G. Li
Department of Mechanical Engineering,
University of Sheffield,
Sheffield, S1 3JD, UK

X. Y. Luo
Department of Mathematics,
University of Glasgow,
Glasgow, G12 8QW, UK
e-mail: X.Y.Luo@maths.gla.ac.uk

A. G. Johnson[1]
Academic Surgical Unit,
Royal Hallamshire Hospital,
Sheffield, S10 2JF, UK

N. A. Hill
Department of Mathematics,
University of Glasgow,
Glasgow, G12 8QW, UK

N. Bird
Academic Surgical Unit,
Royal Hallamshire Hospital,
Sheffield, S10 2JF, UK

S. B. Chin
Department of Mechanical Engineering,
University of Sheffield,
Sheffield, S1 3JD, UK

One-Dimensional Models of the Human Biliary System

This paper studies two one-dimensional models to estimate the pressure drop in the normal human biliary system for Reynolds number up to 20. Excessive pressure drop during bile emptying and refilling may result in incomplete bile emptying, leading to stasis and subsequent formation of gallbladder stones. The models were developed following the group's previous work on the cystic duct using numerical simulations. Using these models, the effects of the biliary system geometry, elastic property of the cystic duct, and bile viscosity on the pressure drop can be studied more efficiently than with full numerical approaches. It was found that the maximum pressure drop occurs during bile emptying immediately after a meal, and is greatly influenced by the viscosity of the bile and the geometric configuration of the cystic duct, i.e., patients with more viscous bile or with a cystic duct containing more baffles or a longer length, have the greatest pressure drop. It is found that the most significant parameter is the diameter of the cystic duct; a 1% decrease in the diameter increases the pressure drop by up to 4.3%. The effects of the baffle height ratio and number of baffles on the pressure drop are reflected in the fact that these effectively change the equivalent diameter and length of the cystic duct. The effect of the Young's modulus on the pressure drop is important only if it is lower than 400 Pa*; above this value, a rigid-walled model gives a good estimate of the pressure drop in the system for the parameters studied.* [DOI: 10.1115/1.2472379]

Keywords: bile flow, cystic duct, gallstone, pressure drop

1 Introduction

Biliary diseases such as cholelithiasis and cholecystitis necessitate surgical removal of the gallbladder (GB), which is the most commonly performed abdominal operation in the West. Some 60,000 operations for gallbladder disease are performed in the UK each year [1] at a cost to the National Health Service (NHS) of approximately £60 million per annum [2]. In order to understand the causes of these diseases, it is important to understand the physiological and mechanical functions of the human biliary system. The human biliary system consists of the gallbladder, cystic duct, common hepatic duct and common bile duct (Fig. 1). The human gallbladder is a thin-walled, pear-shaped sac that measures approximately 7–10 cm in length and ~3 cm in width. Its average storage capacity is 20–30 ml. The human cystic duct is approximately 3.5 cm long and 3 mm wide and merges with the common bile duct. The mucosa of the proximal cystic duct is arranged into 3–7 crescentic folds or valves known as the spiral valves of Heister. The human common duct is normally about 10–15 cm long and 5 mm wide, in which the hepatic common duct is ~4 cm long. The common bile duct merges with the pancreatic duct before entering the duodenum at the ampulla [3,4].

While the anatomical and physiological aspects of the human biliary system have been studied extensively, little is known about flow mechanics in the system. Torsoli and Ramorino [5] measured pressures in the biliary tree and found them to vary from 0–14 cm H_2O (1 cm H_2O=100 Pa) in the resting gallbladder to approximately 12–20 cm H_2O in the common bile duct. Earlier experimental work by Rodkiewicz and Otto [6] showed that bile behaves like a Newtonian fluid, although this has been challenged recently [7–9]. Kimura [10] found that the relative viscosity of bile is between 1.8 and 8.0, while Joel [11] found it is between 1.77 and 2.59. The relative viscosity is defined as the dynamic viscosity of the investigated fluid compared with that of distilled water, both at the same temperature. Tera [12] measured the dynamic viscosity of gallbladder bile by using eight 8-cm-long capillary tubes with a diameter of 0.2 mm. It was found that the normal gallbladder bile was layered and the relative viscosity of the top, thinnest layer was 2.1 and the bottom thickest layer was 5.1. Bouchier et al. [13] also reported that relative viscosity, determined by a capillary flow viscometer, was greater in pathological gallbladder bile than normal gallbladder bile, and both were more viscous than hepatic duct bile. Although the concentration of normal gallbladder bile affected the bile viscosity, in pathological and hepatic bile, the content of mucous was the major factor determining viscosity. Cowie et al. [14] showed that the mean viscosity of bile from gallbladders containing stones was greater than that from healthy ones. The presence of mucous in gallbladders with stones was likely to account for the differences in viscosity based on the viscosity results using a Cannon-Fiske capillary viscometer at room temperature.

The complicated geometry of the biliary tree makes it difficult to estimate the pressure drop during bile emptying using the Poiseuille formula. Rodkiewiz et al. [15] found that flow of bile in the extrahepatic biliary tree of dog was related to the associated pressure drop by a power law and differed from that of laminar flow in a rigid tube. Dodds et al. [16] calculated the volume variations of the gallbladder during emptying using the ellipsoid and sum-of-cylinders methods from the gallbladder images. Jazrawi et al. [17] performed simultaneous scintigraphy and ultrasonography for 14 patients with gallstones and 11 healthy controls and studied the postprandial refilling, turnover of bile, and turnover index. They

[1]Deceased.

Contributed by the Bioengineering Division of ASME for publication in the JOURNAL OF BIOMECHANICAL ENGINEERING. Manuscript received February 1, 2005; final manuscript received October 7, 2006. Review conducted by Ajit Yoganathan.

 Copyright © 2007 by ASME

Downloaded 09 Jun 2007 to 219.245.144.250. Redistribution subject to ASME license or copyright, see http://www.asme.org/terms/Terms_Use.cfm

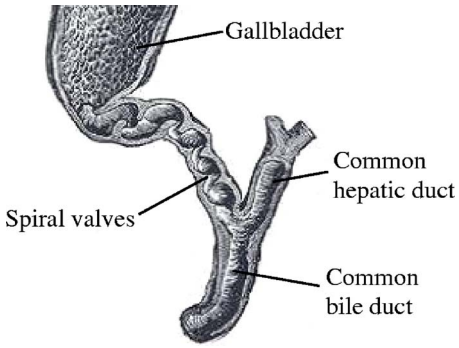

Fig. 1 Gross anatomy of the human biliary tree showing part of the gallbladder neck connected to the spiral valves in the cystic duct [3]

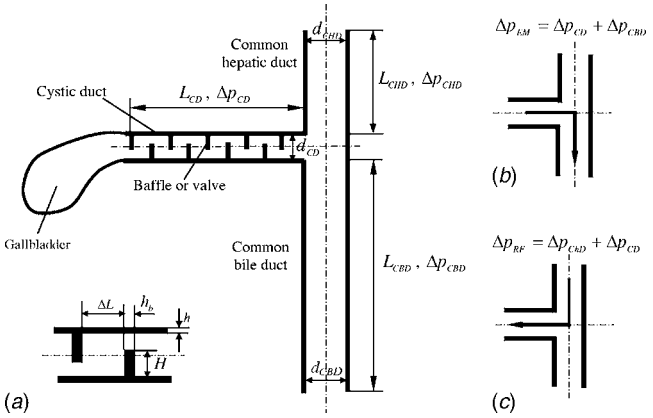

Fig. 2 Schematic geometry model of human billiary system (*a*) and bile flow directions in the (*b*) emptying and (*c*) refill phases

found that in postprandial healthy controls, the gallbladder handles up to six times its basal volume within 90 min, but this turnover of bile is markedly reduced in cholelithiasis causing a reduced washout effect of the gallbladder contents, including cholesterol crystals (They did not actually measure the cholesterol crystals). Deenitchin [18] investigated the relationships between a complex cystic duct and cholelithiasis in 250 patients with cholelithiasis and 250 healthy controls. It was found that the patients with gallstones had significantly longer and narrower cystic ducts than those without stones. The results suggested that complex geometry of the cystic ducts may play an important role in cholelithiasis. An increase in the cystic duct resistance has been shown to result in sludge formation and eventually stones in the gallbladder [19–23]. Recently, Bird et al. [24] have investigated the effects of different geometries and their anatomical functions of the cystic ducts.

It is now generally accepted that prolonged stasis of bile in the gallbladder is a significant contributing factor to gallstone formation, suggesting that fluid mechanics, in particular, the pressure drop that is required to overcome the resistance of bile flow during emptying, may play an important role in gallstone formation. Unusually high gallbladder pressures could be a cause of acute pain observed in vivo, and also indicate that the gallbladder could not empty satisfactorily, increasing the likelihood of forming cholesterol crystals.

Ooi et al. [25] performed a detailed numerical study on flow in two- and three-dimensional cystic duct models. The cystic duct models were generated from patients' operative cholangiograms and acrylic casts. The pressure drops in these models were compared with that of an idealized straight duct with regular baffles or spiral structures. The influences of different baffle heights, numbers, and Reynolds numbers on the pressure drop were investigated. They found that an idealised duct model, such as a straight duct with baffles, gives qualitative measurements that agree with the realistic cast models from two different patients. Experimental work has also been carried out to validate the computational fluid dynamics (CFD) predictions in the simplified ducts [26]. Thus, the simplified models can be used to provide some physical insights into the general influence of cystic duct geometry on the pressure drop [25].

In this paper, in order to obtain a global view of the total pressure drop in the whole biliary system and to consider the importance of the effects of fluid-structure interaction in the human cystic duct, we propose two one-dimensional models of the human biliary system, one with a rigid wall and one with an elastic wall. These models are based on the three-dimensional straight duct with regular baffles used by Ooi et al. [25]. The rigid model is validated against the three-dimensional simulations, and the differences between the elastic and rigid models are discussed. Using these models, the effects of physical parameters such as the cystic duct length, diameter, baffle height ratio, number of baffles, Young's modulus, and the bile viscosity, on the pressure drop are studied in detail. Both refilling and emptying processes are modeled, and the bile flow in the hepatic and common bile ducts is also taken into consideration. It is hoped that these models can be further developed to provide some fast, qualitative estimates of pressure drop based on real time *in vivo* data of patients' biliary systems and therefore be used to aid clinical diagnosis in the longer term.

The remainder of the paper is organized as follows. The characteristics of geometry and flow are described in Sec. 2, and the one-dimensional models are introduced in Sec. 3. The results and discussion are given in Sec. 4, followed by the conclusions.

2 Characteristics of Geometry and Flow

Anatomical descriptions of the biliary system date back to the 18th century when Heister [4] reported spiralling features in the lumen of the cystic duct and called them "valves." Although later researchers doubted the valvular function, the term "valves of Heister" is still in use. The gross anatomy of the biliary system shown in Fig. 2 begins from the gallbladder neck which funnels into a cystic duct. Spiralling mucous membranes are generally prominent in the proximal part of the cystic duct (*pars spiralis or pars convoluta*), which then smoothes out to form a circular lumen at the distal end (pars glabra). Although the actual geometry of the cystic, common hepatic, and bile ducts is very complicated and subject dependent, and the ducts are all curved, to obtain a system view we can schematically represent the human biliary system as in Fig. 2.

The flow directions of the bile during gallbladder emptying immediately after meal, and during refilling are also shown in Fig. 2. Usually, it takes about half an hour for emptying and several hours (until the next meal) for refilling. The gallbladder volume variation with time in both emptying and refilling is shown in Fig. 3 [4]. From this figure, we can derive the corresponding flow rate (or volume flux) Q ($=dV/dt$). For a healthy person, the average bile density ρ is about 1000 kg/m^3, the same as water, and the range of diameter of the cystic duct is about $d_{CD}=1-4$ mm [24]. The temporal acceleration of bile ($\rho\partial u/\partial t$) is approximately 10^{-3}m/s^2 in the emptying phase and 10^{-5}m/s^2 in the refilling, and can therefore be ignored in our model. In addition, the maximum Reynolds number ($\mathrm{Re}=4Q/\pi\nu d_{CD}$) estimated for a cystic duct with diameter of 1 mm and bile kinematical viscosity $\nu=1.275\mathrm{mm}^2/s$ is about 20 during normal emptying, and even smaller during refilling. Hence the flow is laminar. Finally, for a healthy person without gallstones, the bile can be reasonably considered as a Newtonian fluid [25,27].

Downloaded 09 Jun 2007 to 219.245.144.250. Redistribution subject to ASME license or copyright, see http://www.asme.org/terms/Terms_Use.cfm

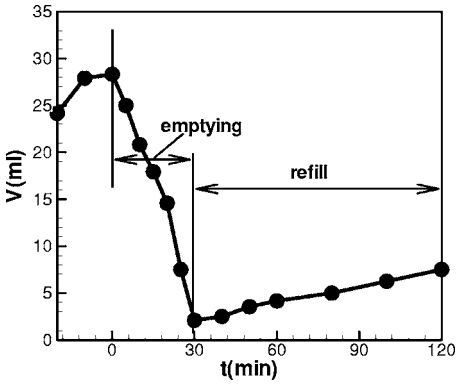

Fig. 3 Gallbladder volume variation with time during emptying and refilling. Note that only part of the refilling phase is plotted.

3 One-Dimensional Models

The pressure drop during emptying is believed to have a link with the stone formation in gallbladder [18]. Our primary aim, therefore, is to predict this pressure drop in a mathematical model of the human biliary system. It is noted that the key structure contributing to the pressure drop is the cystic duct, while the hepatic and common bile ducts offer little resistance or geometric changes during emptying and refilling. Therefore, to simplify the pressure drop prediction, the modeling focuses on the non-linear flow features in the cystic duct, while Poiseuille flow is assumed in the other two biliary ducts. In the following, the effects of the baffles in the cystic duct are considered in order to determine the equivalent diameter and length. The effects of the elastic wall are then considered on a straight model of the cystic duct using the concept of equivalent diameter and length.

3.1 Rigid Wall Model. For a given flow rate, the flow resistance is defined as the pressure drop required to drive the flow along the duct. This pressure drop generally includes viscous losses and any local flow separation or vortex loss.

3.1.1 Equivalent Diameter and Length. It is assumed that the common bile duct and the common hepatic duct are straight tubes and join at a T-junction (Fig. 2). To model the effects of the cystic duct baffles on the flow, following Ooi et al. [25], the baffles are arranged in the simplified manner, shown in Fig. 4. Unlike in the straight tube, the flow in the cystic duct needs to negotiate its way around the baffles and the worst scenario is shown by the arrow in Fig. 4. Thus the key problem is to estimate the equivalent length L_{eq}, and the equivalent diameter d_{eq}, treating the cystic duct as an "equivalent straight pipe." Once this is done, it is straightforward to calculate the pressure drop in the cystic duct assuming Poiseuille flow.

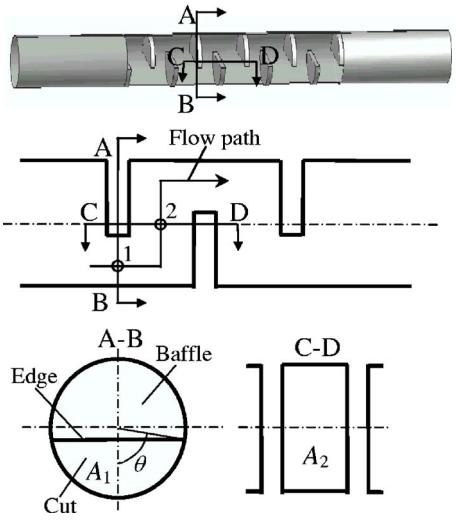

Fig. 4 Baffle and cross sections of duct. A_1 is the cross-sectional area of flow at point 1, and A_2 the cross-sectional area of the flow at point 2.

The equivalent diameter for the cystic duct (d_{CD}), is dependent on the number of baffles, as well as the baffle height. From Fig. 4 we can see that the bile flow travels twice the distance from points 1 to 2 between any two baffles in the duct, and A_1 and A_2 are the corresponding cross-sectional areas at points 1 and 2. The sector area A_1 can be easily calculated from

$$A_1 = d_{CD}^2\theta/4 - \sqrt{d_{CD}^2/4 - (H - d_{CD}/2)^2}(H - d_{CD}/2) \tag{1}$$

where θ is half of the center angle of the baffle cut, and is written as

$$\theta = \begin{cases} \tan^{-1}[\sqrt{d_{CD}^2/4 - (H - d_{CD}/2)^2}/(H - d_{CD}/2)] & H > d_{CD}/2 \\ \pi/2 & H = d_{CD}/2 \\ \pi + \tan^{-1}[\sqrt{d_{CD}^2/4 - (H - d_{CD}/2)^2}/(H - d_{CD})] & H < d_{CD}/2 \end{cases} \tag{2}$$

for a given tube with fixed values of L_{CD} and d_{CD}, A_1 depends on the baffle height H only.

The maximum diameter of the flow passage is equal to the diameter of cystic duct d_{CD} without baffles, i.e.,

$$d_{eq,max} = d_{CD} \tag{3}$$

It is shown in the appendix that for the range of parameters in which we are interested, A_1 is always smaller than A_2. Therefore, the minimum diameter of the flow passage is associated with A_1, i.e.,

$$d_{eq,min} = 2\sqrt{A_1/\pi} \tag{4}$$

We now assume that the equivalent diameter of cystic duct varies linearly with the number of baffles between $d_{eq,min}$ and $d_{eq,max}$, i.e.,

$$d_{eq} = d_{eq,min} + (d_{eq,max} - d_{eq,min})\left(1 - \frac{n}{n_c}\right) \tag{5}$$

where n_c is the maximum number of baffles considered. For the parameters we considered, $n_c = 18$ (for details, see appendix).

The equivalent length of the cystic duct is determined from the actual length of the flow passage along the duct plus an extra length due to the complicated flow pattern, i.e.,

$$L_{eq} = H(n - 1) + L_{CD} + L_m \tag{6}$$

where L_m denotes the extra length corresponding to the minor pressure drop due to local vortices from the cross-sectional area expansion, contraction, and the flow path bending in the baffle zone. It can be estimated from [28] that

$$L_m = \frac{\pi d_{eq}^4 \Delta p_m}{128\mu Q} \tag{7}$$

where Δp_m is the local pressure drop predicted by Bober and Kenyon [29], i.e.,

$$\Delta p_m = 16n(c_1 + c_2)\frac{\rho Q^2}{\pi d_{eq,min}^4} + 16c_3(n - 1)\frac{\rho Q^2}{\pi d_{eq,min}^4} \tag{8}$$

Here, the sudden contraction head-loss coefficient is $c_1 = 0.42(1 - A_1/A_{CD})$, and the sudden expansion head-loss coefficient is $c_2 = (1 - A_1/A_{CD})^2$ [28]. The coefficient c_3 is the head-loss due to the flow bending around the baffles and it is a function of the bending angle. For a 90 deg bend, c_3 has been measured to be 0.75 [29]. In our model, the angle through which the flow bends around a baffle should depend largely on the baffle height ratio ξ, and to a lesser

Downloaded 09 Jun 2007 to 219.245.144.250. Redistribution subject to ASME license or copyright, see http://www.asme.org/terms/Terms_Use.cfm

extent, on the number of baffles as well. For simplicity, however, we assume that the angle is a linear function of ξ, i.e., $c_3=k\xi$, where k is chosen to be 0.85. Thus, for $\xi=0$ (straight tube flow), $c_3=0$ and for $\xi=0.9$, where 3D simulations typically show that the flow turning through 90 deg around the baffles, $c_3=0.75$.

3.1.2 Emptying Phase. The pressure drop in the cystic duct in the emptying phase for a given number of baffles can now be estimated for Poiseuille flow [28]

$$\Delta p_{\mathrm{CD}} = \frac{128\mu Q}{\pi d_{\mathrm{eq}}^4} L_{\mathrm{eq}} \tag{9}$$

For the common bile duct, in the emptying phase, the pressure drop can be written as

$$\Delta p_{\mathrm{CBD}} = \frac{128\mu Q}{\pi d_{\mathrm{CBD}}^4} L_{\mathrm{CBD}} + \Delta p_{te} \tag{10}$$

where Δp_{te} accounts for the pressure drop owing to the T-junction, which consists of one 90 deg bend and one expansion, given

$$\Delta p_{te} = 16c_4 \frac{\rho Q^2}{\pi^2 d_{\mathrm{CD}}^4} + 16c_2 \frac{\rho Q^2}{\pi^2 d_{\mathrm{CD}}^4} \tag{11}$$

The coefficients $c_4=0.75$ for a 90 deg bend and c_2 may be treated in the same manner as those for Eq. (8). Thus, the total pressure drop in the biliary system during the emptying phase is

$$\Delta p_{\mathrm{EM}} = \frac{128\mu Q}{\pi d_{\mathrm{eq}}^4} L_{\mathrm{eq}} + \frac{128\mu Q}{\pi d_{\mathrm{CBD}}^4} L_{\mathrm{CBD}} + \Delta p_{te} \tag{12}$$

3.1.3 Refilling Phase. Likewise, during refilling, the pressure drop in the common bile duct is expressed by Eq. (10), and the pressure drop in the common hepatic duct is

$$\Delta p_{\mathrm{CHD}} = \frac{128\mu Q}{\pi d_{\mathrm{CHD}}^4} L_{\mathrm{CHD}} + \Delta p_{th} \tag{13}$$

where

$$\Delta p_{th} = 16c_4 \frac{\rho Q^2}{\pi^2 d_{\mathrm{CHD}}^4} + 16c_1 \frac{\rho Q^2}{\pi^2 d_{\mathrm{CHD}}^4} \tag{14}$$

and the total pressure drop during refilling is

$$\Delta p_{\mathrm{RF}} = \frac{128\mu Q}{\pi d_{\mathrm{eq}}^4} L_{\mathrm{eq}} + \frac{128\mu Q}{\pi d_{\mathrm{CHD}}^4} L_{\mathrm{CHD}} + \Delta p_{th} \tag{15}$$

3.2 Elastic Wall Model. In order to obtain a more realistic description for the pressure drop in the human biliary system, an elastic wall model is now considered. In reality, the ducts are soft tissues made of nonlinear material, i.e., Young's modulus varies with the internal pressure [30,31]. However, in the first instance, it is assumed that the cystic duct is a linear, isotropic elastic material with a uniform wall thickness. The hepatic and common bile ducts are still assumed to be rigid for two reasons: one is that Young's modulus of these ducts is greater than that of the cystic duct [30]; the other is that the pressure variations in these two ducts are much smaller (less than 1 Pa) than in the cystic duct and, the deformation of the ducts is much smaller.

For simplicity, we model the elastic behavior of the cystic duct as an "equivalent pipe" with an equivalent length $L=L_{\mathrm{eq}}$, and a diameter d_{eq}. In other words, the effects of baffles on the flow come implicitly through L_{eq} and d_{eq} (or area A_{eq}, which varies with the transmural pressure, i.e., internal minus external). We assume that the cystic duct is initially circular and the duodenal valve opens during emptying, which reduces the pressure in the common bile duct. This, together with the rise in the gallbladder pressure, will initiate the bile flow out of the gallbladder, which further decreases the pressure downstream in the cystic duct. Thus, the transmural pressure in the downstream part of the cystic duct during emptying will become negative. As a result, the cystic duct becomes partially collapsed towards the downstream end. This fluid-structure behavior is modeled following well-known work on collapsible tube flows [32–34].

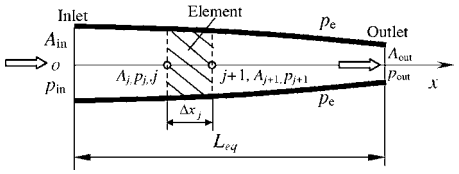

Fig. 5 A simplified cystic duct in the emptying phase. The duct is initially circular at the inlet, and the downstream part collapses due to the pressure drop as bile flows.

3.2.1 Elastic Wall Model

3.2.1.1 Emptying phase. The partially collapsed cystic duct is shown schematically in Fig. 5, where p_e is the external pressure, and equals the pressure in the chest, i.e., $p_e=1.5$ kPa [4] (above atmospheric pressure). We introduce a one-dimensional coordinate system originating from point "O." As the bile flows down the cystic duct, the internal pressure decreases due to viscous losses, causing a decrease in transmural pressure $(p-p_e)$ from the inlet (A_{in}) to the outlet (A_{out}). The governing equations for the tube flow in the elastic cystic duct are [32]

$$Q = Au \tag{16}$$

$$\rho u \frac{du}{dx} = -\frac{dp}{dx} - \frac{8\pi\mu Q}{A^2} \tag{17}$$

The pressure at the inlet is chosen as the reference pressure. For a given flow rate, the corresponding pressure in the duct is derived by integrating Eq. (17)

$$p = p_{\mathrm{in}} - 8\pi\mu Q \int_0^x \frac{1}{A^2(x')} dx' + \frac{1}{2}\rho Q^2 \left(\frac{1}{A_{\mathrm{in}}^2} - \frac{1}{A^2} \right) \tag{18}$$

The constitutive equation for the duct with an elastic wall obeys the "tube law" for homogeneous elastic materials [33]

$$p - p_e = K_p F(\alpha) \tag{19}$$

where

$$K_p = \frac{Eh^3}{12(1-\sigma^2)r^3} \tag{20}$$

and $\alpha=A/A_0$. $F(\alpha)$ is usually determined by experiment. For veins, the tube law can be expressed as [32,34]

$$F(\alpha) = \alpha^{10} - \alpha^{-3/2} \tag{21}$$

Since there are no experimental data for the cystic duct, here we assume that it obeys Eq. (21). The fluid pressure estimated using Eq. (19) is

$$p = p_e + \frac{\pi^{3/2} Eh^3}{12(1-\sigma^2)A^{3/2}} [\alpha^{10} - \alpha^{-3/2}] \tag{22}$$

Combining Eqs. (18) and (22), we have

$$p_{\mathrm{in}} - 8\pi\mu Q \int_0^x \frac{1}{A^2} dx' + \frac{1}{2}\rho Q^2 \left(\frac{1}{A_{\mathrm{in}}^2} - \frac{1}{A^2} \right) = p_e + \frac{\pi^{3/2} Eh^3}{12(1-\sigma^2)A^{3/2}} [\alpha^{10} - \alpha^{-3/2}] \tag{23}$$

Equation (23) represents a one-dimensional boundary value problem, which is solved using a finite difference method. The duct is divided into J elements (J is chosen to be >300); a typical element extending from node j to $j+1$ is illustrated in Fig. 5. At the $(j+1)$th node

Downloaded 09 Jun 2007 to 219.245.144.250. Redistribution subject to ASME license or copyright, see http://www.asme.org/terms/Terms_Use.cfm

Table 1 A summary of parameters for human biliary system

Cystic duct	d_{CD}=1–6 mm, L_{CD}=40 mm, $h=h_b$=0.5 mm, ξ=0.3–0.7, n=0–18, σ=0.5, E=100–1000 Pa
Common bile duct	d_{CBD}=6 mm, L_{CBD}=100 mm
Common hepatic duct	d_{CHD}=40 mm, L_{CHD}=40 mm
Bile	ρ=1000 kg/m^3, υ=1–3 mm^2/s

$$p_j + \frac{1}{2}\rho Q^2\left(\frac{1}{A_j^2} - \frac{1}{A_{j+1}^2}\right) - 8\pi\mu Q\left(\frac{1}{A^2}\right)_{j+1/2}\Delta x_j = p_e + \frac{\pi^{3/2}Eh^3}{12(1-\sigma^2)A_{j+1}^{3/2}}\left[\left(\frac{A_{j+1}}{A_0}\right)^{10} - \left(\frac{A_{j+1}}{A_0}\right)^{-3/2}\right] \quad (24)$$

where

$$p_j = p_{in} - 8\pi\mu Q\int_0^{x_j}\frac{1}{A^2}dx + \frac{1}{2}\rho Q^2\left(\frac{1}{A_{in}^2} - \frac{1}{A_j^2}\right)$$

$$\left(\frac{1}{A^2}\right)_{j+1/2} = \frac{1}{2}\left(\frac{1}{A_j^2} + \frac{1}{A_{j+1}^2}\right)$$

$$p_{j+1} = p_j + \frac{1}{2}\rho Q^2\left(\frac{1}{A_j^2} - \frac{1}{A_{j+1}^2}\right) - 8\pi\mu Q\left(\frac{1}{A^2}\right)_{j+1/2}\Delta x_j$$

and p_j is known. Expressing $(1/A^2)_{j+1/2}$ in terms of A_j and A_{j+1}, Eq. (24) can also be written as

$$p_j + \frac{1}{2}\rho Q^2\left(\frac{1}{A_j^2} - \frac{1}{A_{j+1}^2}\right) - 4\pi\mu Q\left(\frac{1}{A_j^2} + \frac{1}{A_{j+1}^2}\right)\Delta x_j = p_e + \frac{\pi^{3/2}Eh^3}{12(1-\sigma^2)A_{j+1}^{3/2}}\left[\left(\frac{A_{j+1}}{A_0}\right)^{10} - \left(\frac{A_{j+1}}{A_0}\right)^{-3/2}\right] \quad (25)$$

We employ the bisection method to solve Eq. (25) to find unknown A_{j+1} in region $A_{j+1}\in[0.1A_0, 2A_0]$ in an iterative manner.

The boundary conditions are applied at the inlet (node 1)

$$\begin{cases}\alpha_{in} = A_{in}/A_0 \\ p_{in} = p_e + \dfrac{\pi^{3/2}Eh^3}{12(1-\sigma^2)A_{in}^{3/2}}(\alpha_{in}^{10} - \alpha_{in}^{-3/2})\end{cases} \quad (26)$$

If $\alpha_{in}=1$, then $p_{in}=p_e$; else if $\alpha_{in}>1$, then $p_{in}>p_e$. The maximum pressure drop in the cystic duct is thus $\Delta p_{CD}=p_{in}-p_{out}$, and the total pressure drop occurring during emptying is

$$\Delta p_{EM} = \Delta p_{CD} + \frac{128\mu Q}{\pi d_{CBD}^4}L_{CBD} + \Delta p_{te} \quad (27)$$

3.2.1.2 Refilling phase. Because the bile flow rate is very small during refilling and the refill time is at least three times longer than the emptying time, the cystic duct wall can be regarded as rigid during this phase. Equations (13)–(15) in the rigid model are applied to calculate the pressure drop.

4 Results and Discussion

4.1 Parameters. The parameters used in the models are listed in Table 1. Most of these are taken from the statistics of human ducts given by Deenitchin et al. [18]. The range of values for ξ, n, and d_{CD} are chosen to be the same as in the 3D models by Ooi [25]. The gallbladder flow rate is derived from the volume-time curve in Fig. 3, which lies between 0.49 and 1.23 ml/min. The range of Young's modulus used for this model is based on the measurements of [30], where bile ducts from 16 healthy adult dogs were tested with a pressure ranging from 4.7 kPa to 8 kPa. In fact, the physiological internal pressure is normally around 1.5 kPa in the human biliary system, which is outside the pressure range used by Jian and Wang [30]. In order to obtain meaningful results, we estimate Young's modulus for the pressure around 1.5 kPa from the extrapolation of the best curve fitting from the data of [30]. The Young's modulus chosen for the models is therefore in the range of 100 and 1000 Pa, which corresponds to the internal pressure varying from 1.03 to 1.9 kPa.

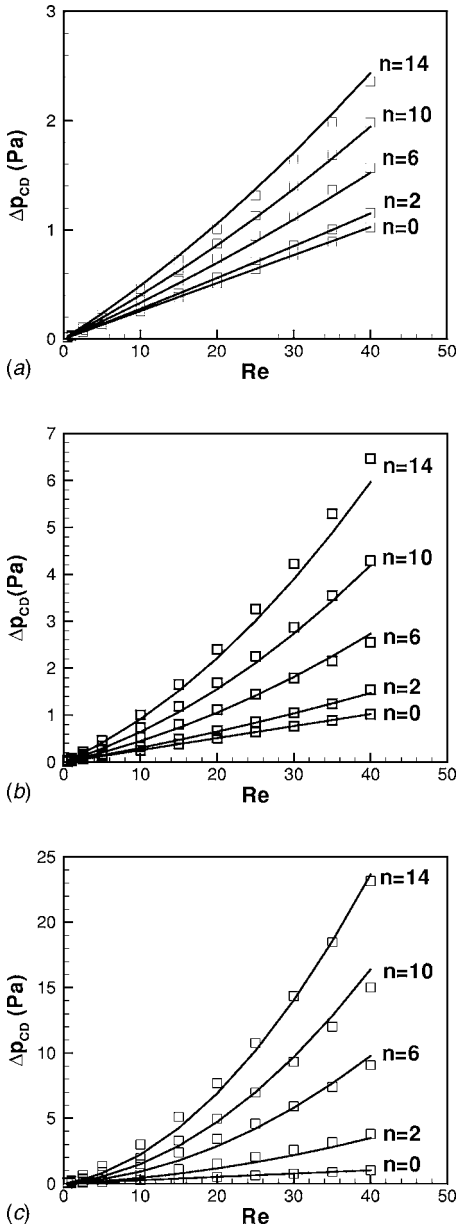

Fig. 6 Comparison of the pressure drop estimated using the 1D rigid model (solid line) and the 3D numerical simulations (symbols). The 3D geometries of the cystic duct are taken from [25].

4.2 One-Dimensional Model Validation. As several assumptions are used in deriving the equivalent diameter and length of the one-dimensional (1D) model, here we compare our 1D model with the three-dimensional (3D) rigid cystic duct models solved with the numerical methods. Figure 6 illustrates the pressure drop variations with Reynolds number using the rigid model for the cystic duct only, with and without baffles. The geometry and bile parameters are L_{CD}=50 mm, d_{CD}=5 mm, n=0, 2, 6, 10, and 14, $h=h_b$=1 mm, ρ=1000 kg/m^3, ν=1 mm^2/s, respectively. These results are compared with the corresponding 3D cystic duct CFD results provided by [25], which was quantitatively validated by

Downloaded 09 Jun 2007 to 219.245.144.250. Redistribution subject to ASME license or copyright, see http://www.asme.org/terms/Terms_Use.cfm

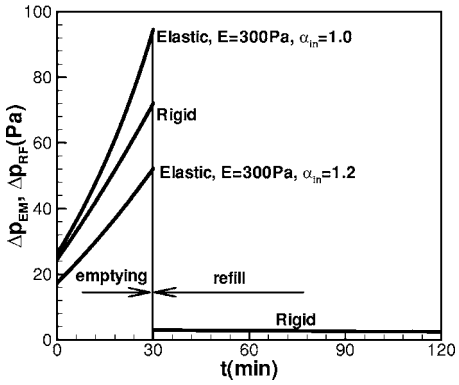

Fig. 7 Pressure drop variation with time predicted using both rigid and elastic 1D models, all other parameters are chosen to be those in the Reference Set

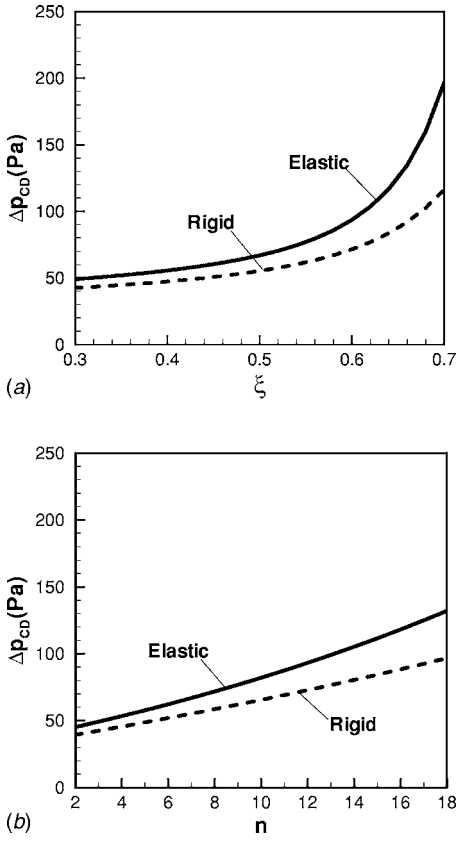

Fig. 8 Pressure drop variations with (*a*) baffle height ratio ξ, and (*b*) number of baffle *n*. All other parameters are chosen to be those in the Reference Set.

experiments [26] for higher Reynolds numbers. It can be seen that the agreement between the rigid model and 3D CFD results is consistently good for all values of parameters. This suggests that we have captured the main features of the flow in the rigid cystic duct. The elastic model is derived for a straight pipe with equivalent diameter and length to the duct with baffles, and is based on the experimental curve for a straight rubber tube [32]. Therefore, if the rigid model with the correct equivalent diameter and length is accepted as satisfactory, then the elastic model is likely to be satisfactory.

4.3 Pressure Drop for the Reference Parameter Set. There are many parameters present in the model, and each can vary within its own physiological range. In order to isolate the effect of each individual parameter, we introduce a Reference Parameter Set (henceforth referred to as the Reference Set), which is based on averaged values of a normal human cystic duct. The Reference Set is: $n=7$, $\xi=0.5$, $\nu=1.275$ mm^2/s, $d_{CD}=1$ mm, $L_{CD}=40$ mm, $E=300$ Pa, $\alpha_{in}=1$, and $Q=1$ ml/min. The effect of any particular parameter on the pressure drop is determined by varying this parameter while keeping all the other parameters fixed. For the rigid tube, all parameters are the same except that Young's modulus does not apply.

The predicted pressure drops in the human biliary system using the rigid and elastic models are shown in Fig. 7. Two cases are considered: $\alpha_{in}=1$ and 1.2. $\alpha_{in}=1$ is the case when the inlet of the cystic duct is not expanded, while $\alpha_{in}=1.2$ indicates a duct expansion sometimes observed clinically. It can be seen that for $\alpha_{in}=1$, the elastic model predicts a greater pressure drop in the emptying phase, due to the collapse of the cystic duct. It is also noted that the maximum value of the pressure drop agrees with the typical physiological observation of 20 to 100 Pa [4,35].

The ratio of total pressure drop in the common bile duct or common hepatic duct to the total pressure drop in the cystic duct can illustrate the importance of the pressure drop across the cystic duct in the human biliary system. The results demonstrate that the pressure drop in the common duct is less than 1.5%, and in the common hepatic duct less than 0.15% only, compared to that in the cystic duct. This justifies estimating the pressure drop in the human biliary system from the cystic duct model only, as was done by Ooi et al. [25].

In the following, the pressure drop in the cystic duct is presented in the results. All the parameters used below are in those in the Reference Set unless otherwise stated.

4.4 Effects of Parameters on the Pressure Drop. The effects of the baffle height ratio ξ and number of baffles n on the pressure drop are shown in Fig. 8. The pressure drop predicted by the elastic model is also compared with the corresponding rigid model. The pressure drop increases as ξ increases since the greater the baffle height ratio, the narrower the equivalent diameter. As ξ varies from 0.3 to 0.7, the pressure drop increases from 50 to 100 Pa and 200 Pa for the rigid and elastic ducts, respectively. The pressure drop also increases as n varies from 2 to 18. Over the ranges of parameters chosen in this study, the change in ξ produces a greater change in pressure drops for both rigid and elastic ducts (from approximately 50 to 200 Pa) than the change (from approximately 50 to 100 Pa) in ducts by varying n (Fig. 8). This finding agrees with the numerical observations by Ooi et al. [25]. In addition, the pressure drop predicted by the elastic wall model is always greater than that estimated by the rigid wall model for all values of ξ and n, due to the duct collapsing downstream (see Fig. 10 below), which effectively reduces d_{eq}.

Figure 9 demonstrates the pressure drop variations with the cystic duct diameter d_{CD} and bile viscosity ν. The diameter has the strongest effect on the pressure drop. A narrow diameter causes a dramatic increase in pressure drop, as shown in Fig. 9, and 1% decrease in d_{CD} gives rise to 2.7%–4.3% increases in the pressure drop. As the bile viscosity increases from 1 to 3mm^2/s, the pressure drop rises. This increase is greatly augmented by the elastic duct, since the elastic duct collapses downstream (Fig. 10), which causes a nonlinear variation of the pressure drop with the viscosity. The fact that the bile viscosity can also lead to a great increase in the pressure drop supports the clinical observations that an increased bile viscosity may relate to the possible formation of gallbladder stones. Indeed, Jungst et al. [9] have found that the viscosity of bile is markedly higher in the patients with cholesterol stones (5.0 m Pa s) compared to hepatic bile (0.92 m Pa s) in healthy ones.

The effects of varying Young's modulus on the cystic duct and the bile flow rate are shown in Fig. 10, where the pressure drop and the maximum cross-sectional area ratio are plotted against

Downloaded 09 Jun 2007 to 219.245.144.250. Redistribution subject to ASME license or copyright, see http://www.asme.org/terms/Terms_Use.cfm

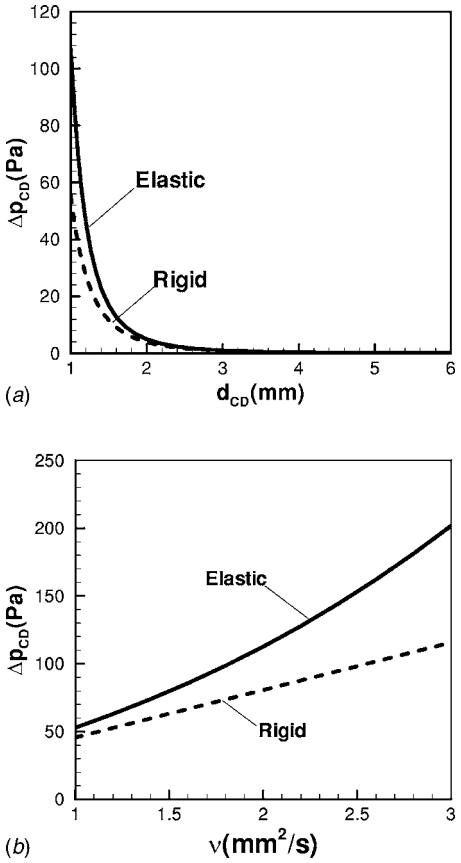

Fig. 9 Pressure drop variations with (*a*) cystic duct diameter d_{CD} and E=100 Pa, and (*b*) bile viscosity ν and E=300 Pa. All other parameters are chosen to be those in the Reference Set.

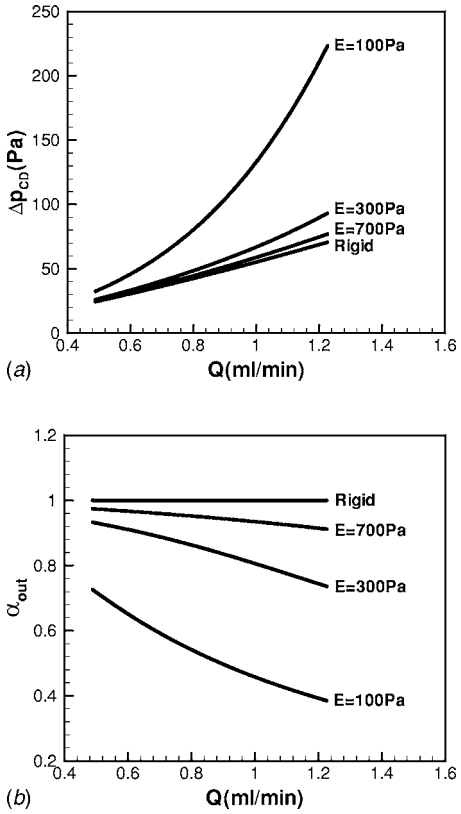

Fig. 10 Variation of (*a*) the pressure drop Δp_{CD} and (*b*) the area ratio α_{out} with flow rate for various values of Young's modulus. All other parameters are chosen to be those in the Reference Set.

flow rate for various values of Young's modulus. It can be seen that a lower Young's modulus (i.e., a more compliant duct) causes a greater pressure drop and a reduction in α. A value of $\alpha_{out}<1$ indicates the duct is collapsed at the downstream end, as α_{out} is the area ratio of the duct outlet to inlet. As Young's modulus is decreased from 700 Pa to 100 Pa, α_{out} decreases from 0.94 to 0.4 at the flow rate of 1.23 ml/min. This is because a cystic duct with a smaller Young's modulus collapses more during the emptying phase. On the other hand, as Young's modulus is greater than 700 Pa, its effect on the pressure drop is almost negligible.

Figure 11 illustrates the pressure drop relation with Young's modulus. It can be seen that the pressure drop increases as the Young's modulus decreases. As the modulus varies from 1000 to 100 Pa, the pressure drop increases from 60 to 130 Pa.

4.5 The Darcy Friction Factor. To gain more understanding to the results obtained, the Darcy friction factor [28] is chosen as a dimensionless parameter to show the effects of the parameters on the pressure drop. The Darcy factor varies with the geometrical similarity and Reynolds number of the flow. If the geometry of two flows is similar, the friction factor is the same at any Reynolds number. Otherwise, it will differ from each other. When the baffle height and number of baffles vary, the equivalent diameter and length will be modified, then the geometrical similarity of the cystic duct will be destroyed; as a result, the corresponding friction factor will change its value. The Darcy friction factor for our models is defined as [28]

$$f = \Delta p_{CD}\left(\frac{64}{\mathrm{Re}}\right) \Big/ \left(\frac{128\mu Q L_{eq}}{\pi d_{eq}^4}\right) \tag{28}$$

where the Reynolds number is $\mathrm{Re}=4Q/\pi\nu d_{eq}$. 64/Re is the friction factor for a straight circular pipe, denoted by f_{id}, the friction factor ratio is then

$$f/f_{id} = \Delta p_{CD} \Big/ \left(\frac{128\mu Q L_{eq}}{\pi d_{eq}^4}\right) \tag{29}$$

The ratio f/f_{id} indicates the pressure drop in a cystic duct with baffles differs from that in an ideal pipe. When Δp_{CD} obeys Poiseuille's formula, $f/f_{id}=1$, otherwise $f/f_{id}>1$.

Figure 12 illustrates the friction factor ratio f/f_{id} variation with Reynolds number for cystic duct with both rigid and elastic walls for two different values of n and ξ. All the curves take values greater than 1. In general, the friction ratio increases with the number of baffles, and this is further augmented by having an elastic wall, especially at a large Reynolds number. The greatest difference in of f/f_{id} between the cases $n=2$ and $n=18$ for the

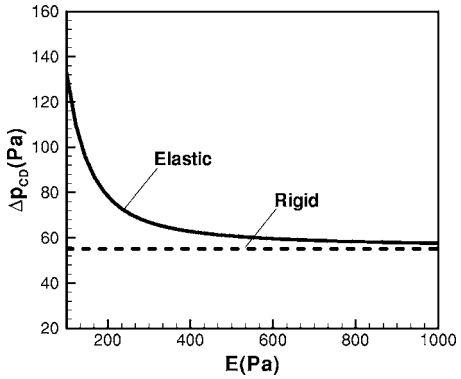

Fig. 11 Variation of pressure drop Δp_{CD} with Young's modulus. All other parameters are chosen to be those in the Reference Set.

Downloaded 09 Jun 2007 to 219.245.144.250. Redistribution subject to ASME license or copyright, see http://www.asme.org/terms/Terms_Use.cfm

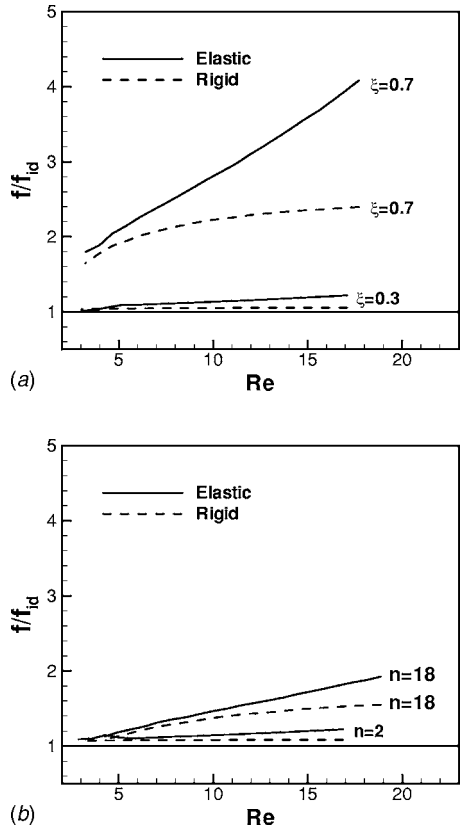

Fig. 12 Variation of the friction factor ratio with Reynolds number for cystic duct with rigid and elastic wall for (*a*) ξ=0.3 and 0.7 and (*b*) *n*=2 and 18. All other parameters are chosen to be those in the Reference set.

rigid duct is approximately 0.4, and for the elastic duct it is approximately 0.6 (Fig. 12(*b*)). In contrast, the greatest difference in f/f_{id} between the cases ξ=0.3 and 0.7 is approximately 1.4 for the rigid duct and 2.9 for the elastic ducts. This supports our previous observation that the influence of baffle height ratio on the pressure drop is greater than the number of baffles. The main reason for this is that the baffle height causes more changes in both the equivalent diameter and the equivalent length. Detailed changes of the equivalent diameter and length by the baffle height and number are listed in Table 2.

It is difficult to compare our results quantitatively to the clinical observations of gallstones due to limited experimental data to date. However, several of experimental studies support our results. Gallstone formation is closely related to the cystic duct resistance or the pressure drop [19] because the resistance or drop can cause bile stasis in gallbladder. Deenitchin et al. [18] has illustrated that the patients with gallstones tend to have long and narrow cystic ducts. Jeffrey et al. [34] found that gallbladder stasis is also related to hyper-secretion of gallbladder mucus for liver, which contributes to an increase in bile viscosity [9]. These are in agreement with our findings. The results from the elastic models cannot be related directly to any clinical observations due to the complete absence of available data; however, our results suggest that for Young's modulus greater than 700 Pa, the rigid model serves as a good approximation to the mechanical behavior of the cystic duct.

Table 2 Equivalent diameter and length

Case 1, n=7			Case 2, ξ=0.5		
ξ	d_{eq} (mm)	I_{eq} (mm)	n	d_{eq} (mm)	L_{eq} (mm)
0.3	0.97–5.48	44.1–52.7	2	0.98–5.79	43.2–45.4
0.5	0.95–5.18	53.0–64.7	7	0.95–5.18	53.1–64.7
0.7	0.94–5.13	105.9–107.4	18	0.88–3.89	68.3–96.7

The combined effects on the pressure drop from all the parameters can be best represented by the friction factor ratio from Eq. (29). Any increase of the ratio above the unity caused by a specific parameter indicating the specific increase in the pressure drop (or resistance) by that parameter. In fact, if all geometrical facts are converted to the equivalent diameter and length, then Eq. (29) can be used to describe precisely the impact of these parameters on the friction ratio (i.e., the nondimensionless pressure drop). In other words, the equivalent diameter d_{eq} is undoubtedly the most significant effect of all, because the friction ratio is proportional to d_{eq}^4.

The diameter of the cystic duct in the Reference Set is chosen to be 1 mm, which is on the smaller side of the measured range [24]. This is because we have not taken into consideration the taper of the duct. In addition, when a cast of the cystic duct is made, there is some degree of dilation, the values measured from the casts are likely to be greater than these of in vivo. Throughout this paper, bile is assumed to be a Newtonian fluid; i.e., its viscosity is independent of the shear rate. However, recent experimental studies suggest that bile may display non-Newtonian behavior such as shear thinning [6–9]. In addition, tests that were carried out in our laboratory on fresh human bile after operations seem to suggest that the degree of the non-Newtonian behavior of bile is not only subject dependent, but also serves as an indication of whether crystals are present in the biliary system. In other words, bile from normal subjects is more likely to be Newtonian [27]. As our main purpose here is to identify possible indicators of gallstone formation for initially healthy subjects before any pathological changes have occurred, it is reasonable to use a Newtonian fluid to represent bile. However, to further develop the model for the diagnosis of individual patients in future, it is important that the non-Newtonian properties of the bile or perhaps a two-phase flow model are considered.

5 Conclusions

One-dimensional rigid and elastic wall models have been proposed for estimating the pressure drop in the human biliary system. Using this model, the effects of the geometry, elasticity of cystic duct wall, bile flow rate and viscosity on the pressure drop were studied in detail. The effect of a particular parameter on the pressure drop is studied by varying this parameter alone while fixing other parameters as those in the Reference Set. It is evident that the most significant parameter is the diameter of the cystic duct. If the viscosity ν is varied from 1–3 mm^2/s, the pressure drop will increase to two times for rigid model and up to four times for the elastic model. While varying the baffle height ratio will cause the pressure drop to be up to two/four times higher for the rigid/elastic models. Increase the number of baffle can also increase the pressure drop in both rigid and elastic ducts, though to a lesser extent compared to the effect of the baffle height ratio. These two geometric parameters affect the pressure drop effectively through the changing of the equivalent diameter, as shown in Table 2; their effects are also shown quantitatively by plotting the Darcy friction ratio. Clearly, the elasticity of the duct plays an important role here. With all other parameters fixed in the Reference set, as Young's modulus decreases from 1000 to 100 Pa, the pressure drop increases to be more than two times higher. However, it was found that when Young's modulus of the cystic duct is more than 700 Pa, a rigid-walled model gives a good estimate of the pressure drop in the system.

Acknowledgment

We thank SWANN-MORTON Foundation for their financial support for this research.

Downloaded 09 Jun 2007 to 219.245.144.250. Redistribution subject to ASME license or copyright, see http://www.asme.org/terms/Terms_Use.cfm

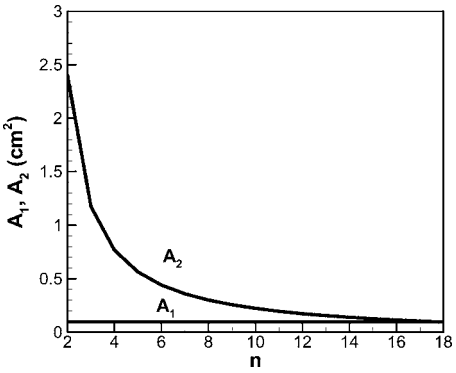

Fig. 13 Variation of A_1 and A_2 with the number of baffles n.

Nomenclature

A = cross-sectional area of collapsed duct, m^2
A_0 = cross-sectional area of duct at zero transmural pressure, m^2
A_1 = cross-sectional area of flow at point 1 in Fig. 4, m^2
A_2 = cross-sectional area of the flow at point 2 in Fig. 4, m^2
c_1 = sudden contraction head-loss coefficient
c_2 = sudden expansion head-loss coefficient
c_3 = head loss coefficient in a bend
c_4 = head loss coefficient in a 90° bend
d = inner diameter of duct, mm
E = Young's modulus of materials, Pa
f = Darcy friction factor
h = thickness of wall or baffle, mm
H = baffle height, mm
j = number of node
J = maximum number of element
K_p = stiffness of wall, Pa
L = length of duct, m
L_m = equivalent length due to minor pressure loss, m
n = number of baffles
n_c = maximum number of baffles
p = internal duct pressure, Pa
p_e = external duct pressure, Pa
Q = bile flow rate, ml/min
Re = Reynolds number, $\mathrm{Re}=ud/\nu$
r = inner radius of duct, $r=\sqrt{A/\pi}$, m
t = time, min
u = bile velocity in cystic duct, $u=Q/A$, m/s
V = bile volume in gallbladder, ml
x = duct center-line coordinate, m
α = area ratio, $\alpha=A/A_0$
μ = bile dynamic viscosity, mPa s
ν = bile kinematic viscosity, $\nu=\mu/\rho$, mm^2/s
θ = half of central angle of baffle cut, rad
ρ = density of bile, kg/m^3
σ = Poisson's ratio
ξ = baffle height ratio, $\xi=H/d_{\mathrm{CD}}$
ΔL = distance between two successive baffles in cystic duct, m
Δp = pressure drop, Pa
Δp_m = minor pressure drop in cystic duct, Pa
Δp_{te} = minor pressure drop in T-junction during emptying, Pa
Δp_{th} = minor pressure drop in T-junction during refill, Pa
Δx = interval of element, m

Subscripts

b = baffle
CBD = common bile duct
CD = cystic duct
CHD = common hepatic duct
EM = emptying
eq = equivalent
id = ideal, straight and circular pipe
in = inlet of duct
max = maximum value
min = minimum value
out = outlet of duct
RF = refilling

Appendix: Geometric Details of the Cystic Model With Baffles

Here, A_2 represents the area of the square intersection formed by the plane through the central line of cystic duct and paralleling the baffle edge with two successive baffles as well as the cystic duct wall. A_2 can be written as

$$A_2 = d_{\mathrm{CD}}\Delta L \tag{A1}$$

The space ΔL between the two successive baffles is

$$\Delta L = \frac{L_{\mathrm{CD}} - nh_b}{n-1} \tag{A2}$$

For given values of L_{CD} and h_b, ΔL or A_2 vary with number of baffles only. The values of A_2 can be calculated and plotted as a function of number of baffles n in Fig. 13. As in Ooi et al. [25], the typical geometric parameters representing the average human cystic duct are chosen to be $L_{\mathrm{CD}}=50$ mm, $d_{\mathrm{CD}}=5$ mm, $n=0$ to 18, $h=1$ mm, and $h_b=1$ mm for this plot. The value of A_1, which is independent of n (see Eq. (1)), is also shown. As n increases, A_2 decreases towards A_1. When $A_2=A_1$, the number of baffles will be

$$n_c = (L_{\mathrm{CD}} + A_1/d_{\mathrm{CD}})/(h_b + A_1/d_{\mathrm{CD}}) \tag{A3}$$

Using the parameters given above, (A3) predicts $n_c=18$. As it is very rare for human cystic ducts to have more than the equivalent of 18 baffles, in the model we assume that $A_2>A_1$, so that the minimum equivalent diameter is always estimated from A_1.

References

[1] Lam, C. M., Murray, F. E., and Cuschieri, A., 1996, "Increased Cholecystectomy Rate After the Introduction of Laparoscopic Cholecystectomy," Gut, **38**, pp. 282–284.
[2] Calvert, N. W., Troy, G. P., and Johnson, A. G., 2000, "Laparoscopic Cholecystectomy: A. Good buy? A. Cost Comparison With Small-Incision (Mini) Cholecystectomy," Eur. J. Surg., **166**, pp. 782–786.
[3] Gray, H., and Lewis, W. H., 1918, *Anatomy of the Human Body*, Lea & Febiger, Philadelphia.
[4] Dodds, W. J., Hogan, W. J., and Green, J. E., 1989, "Motility of the Biliary System," in: *Handbook of Physiology: The Gastrointestinal System*, S. G. Schultz, ed., American Physiological Society, Betheda, Maryland, Vol. 1, Section 6, Part 2(28), pp. 1055–1101.
[5] Torsoli, A., and Ramorino, M. L., 1970, "Motility of the Biliary Tract," Rendiconti Romani di Gastro Enterologica, **2**, pp. 67–80.
[6] Rodkiewicz, Cz. M., and Otto, W. J., 1979, "On the Newtonian Behavior of Bile," J. Biomech., **12**, pp. 609–612.
[7] Gottschalk, M., and Lochner, A., 1990, "Behavior of Postoperative Viscosity of Bile Fluid From T-Drainage," Gastroenterol. J., **50**, pp. 65–67.
[8] Coene, P. P. L. O., Groen, A. K., Davids, P. H. P., Hardeman, M., Tytgat, G. N. T., and Huibregtse, K., 1994, "Bile Viscosity in Patients With Biliary Drainge," Scand. J. Gastroenterol. Suppl., **29**, pp. 757–763.
[9] Jungst, D., Niemeyer, A., Muller, I., Zundt, B., Meyer, G., Wilhelmi, M., and del Pozo, R., 2001, "Mucin and Phospholipids Determine Viscosity of Gallbladder Bile in Patients With Gallstones," World J. Gastroenterol., **7**(3), pp. 203–207.
[10] Kimura, T., 1904, "Untersuchungen Der Benschlichen Blasengalle," Dtsch. Arch. Klin. Med., **79**, pp. 274–289.
[11] Joel, E., 1921, "Visco-und Stalagmome Harns," Biochem. Z., **119**, pp. 93–98.
[12] Tera, H., 1960, "Stratification of Human Gallbladder Bile In Vivo," Acta Chir. Scand. Suppl., **256**, Chap. VIII, pp. 45–50.
[13] Bouchier, I. A. D., Cooperband, S. R., and El Kodsi, B. M., 1965, "Mucous Substances and Viscosity of Normal and Pathological Human Bile," Gastroen-

Downloaded 09 Jun 2007 to 219.245.144.250. Redistribution subject to ASME license or copyright, see http://www.asme.org/terms/Terms_Use.cfm

terology, **49**, pp. 343–353.
[14] Cowie, A. G. A., and Sutor, D. J., 1975, "Viscosity and Osmolality of Abnormal Bile," Digestion, **13**, pp. 312–315.
[15] Rodkiewicz, Cz. M., Otto, W. J., and Scott, G. W., 1979, "Empirical Relationships for the Flow of Bile," J. Biomech., **12**, pp. 411–413.
[16] Dodds, W. J., Groh, W. J., Darweesh, R. M., and Lawson, T. L. et al., 1985, "Sonographic Measurement of Gallbladder Volume," Am. J. Roentgenol., **145**(6), pp. 1009–1011.
[17] Jazrawi, R. P., Pazzi, P., Petroni, M. L., and Prandini, N. et al., 1995, "Postprandial Gallbladder Motor Function: Refilling and Turnover of Bile in Health and in Cholelithiasis," Gastroenterology, **102**(3), pp. 582–591.
[18] Deenitchin, G. P., Yoshida, J., Chijiiwa, K., and Tanaka, M., 1998, "Complex Cystic Duct is Associated With Cholelithiasis," HPB Surg., **11**, pp. 33–37.
[19] Pitt, H. A., Doty, J. E., DenBesten, L. et al., 1982, "Stasis Before Gallstone Formation: Altered Gallbladder Compliance or Cystic Duct Resistance?," Am. J. Surg., **143**, pp. 144–149.
[20] Brugge, W. R., Brand, D. L., Atkins, H. L., et al., 1986, "Gallbladder Dyskinesia in Chronic Acalculous Cholecystitis," Dig. Dis. Sci., **31**, pp. 461–468.
[21] Soloway, R. D., Trotman, B. W., and Ostrow, J. D., 1977, "Pigment Gallstones," Gastroenterology, **72**, pp. 167–182.
[22] Wolpers, C., and Hofmann, A. F., 1993, "Solitary Versus Multiple Cholesterol Gallbladder Stones: Mechanism of Formation and Growth," Clin. Investig., **71**, pp. 423–434.
[23] Bennett, F. D., DeRidder, P., Koloszi, W. et al., 1985, "Cholecystokinin Cholescintigraphic Findings in the Cystic Duct Syndrome," J. Nucl. Med., **10**, pp. 1123–1128.
[24] Bird, N. C., Ooi, R. C., Luo, X. Y., Chin, S. B., and Johnson, A. G., 2006, "Investigation of the Functional Three-Dimensional Anatomy of the Human Cystic Duct: A Single Helix?," *Clinical Anatomy*, pp. 528–534.
[25] Ooi, R. C., Luo, X. Y., Chin, S. B., Johnson, A. G., and Bird, N. C., 2004, "The Flow of Bile in the Human Cystic Duct," J. Biomech., **37**(13), pp. 1913–1922.
[26] Al-Atabi, M., Chin, S. B., and Luo, X. Y., 2005, "Flow Structure in Circular Tubes with Segmental Baffles," *Journal of Flow Visualization and Image Processing*, pp. 301–311.
[27] Ooi, R. C., "Modeling Flow of the Bile in the Human Cystic Duct," PhD thesis, University of Sheffield, 2004.
[28] White, F. M., 1999, *Fluid Mechanics*, 4th ed., McGraw-Hill Book Company, New York, pp. 342–373.
[29] Bober, W., and Kenyon, R. A., 1980, *Fluid Mechanics*, John Wiley & Sons, New York, pp. 295–297.
[30] Jian, C. Y., and Wang, G. R., 1991, "Biomechical Study of the Bile Duct System Outside the Liver," Biomed. Mater. Eng., **1**, pp. 105–113.
[31] Duch, B. U., Petersen, J. A. K., and Gregersen, H., 1998, "Luminal Cross Section Area and Tension-Strain Relation of the Porcine Bile Duct," Neurogastroenterol Motil, **10**, pp. 203–209.
[32] Pedley, T. J., Brook, B. S., and Seymour, R. S., 1996, "Blood Pressure and Flow Rate in the Giraffe Jugular Vein," Philos. Trans. R. Soc. London, Ser. B, **351**, pp. 855–866.
[33] Flaherty, J. E., Keller, J. B., Rubinow, S. I., 1972, "Post Buckling Behavior of Elastic Tubes and Rings With Opposite Sides in Contact," SIAM J. Appl. Math., **23**, pp. 446–455.
[34] Cancelli, C., and Pedley, T. J., 1985, "A. Separated-Flow Model for Collapsible-Tube Oscillations," J. Fluid Mech., **157**, pp. 375–404.
[35] Jeffrey, E. D., Pitt, H. A., Kuchenbecker, S. L., Porter-Fink, V., and DenBesten, L., 1983, "Role of Gallbladder Mucus in the Pathogenesis of Cholesterol Gallstones," Am. J. Surg., **145**, pp. 54–61.

Downloaded 09 Jun 2007 to 219.245.144.250. Redistribution subject to ASME license or copyright, see http://www.asme.org/terms/Terms_Use.cfm